Stimulated-Echo Contrast with Hyperpolarized [1-^{13}C]-Pyruvate

P. E. Larson[1], R. Hurd[2], A. B. Kerr[3], R. Bok[1], J. Kurhanewicz[1], and D. B. Vigneron[1]
[1]Radiology and Biomedical Imaging, University of California - San Francisco, San Francisco, CA, United States, [2]Applied Science Laboratory, GE Healthcare, Menlo Park, CA, United States, [3]Electrical Engineering, Stanford University, Stanford, CA, United States

Introduction: A stimulated-echo sequence with high sensitivity to diffusion and flow is shown here to provide a valuable contrast mechanism for hyperpolarized ^{13}C metabolic imaging (1-4). This mechanism can highlight stationary metabolites, while suppressing signal from flowing metabolites. This helps to distinguish whether ^{13}C-pyruvate is converted to ^{13}C-lactate within the tissue or whether the ^{13}C-lactate was produced elsewhere and flowed into the tissue, thus confounding metabolic state assessments (5).

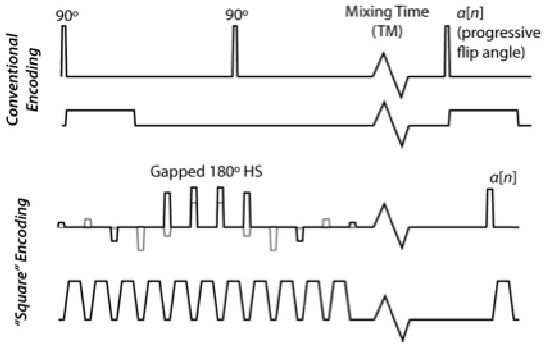

Figure 1: Simulated-echo pulse sequences, including both conventional and square encoding schemes.

Methods: The stimulated-echo (STE) hyperpolarized ^{13}C 3D MRSI pulse sequence we developed consists of a: 1) STE encoding with a dephasing gradient (spin tagging), 2) mixing time (TM) interval allowing for motion, and 3) excitation and rephasing gradient to form STE. Both a conventional (90º-90º) and super-STE (6,7) or "square" encoding were used. The square encoding improves the SNR by storing the magnetization in a square-wave pattern of $+M_0/-M_0$ on the longitudinal axis following the STE encoding, as opposed to the more lossy sinusoidal storage with conventional encoding, but it provides less diffusion encoding strength. A progressive flip angle excitation and EPSI readout gradient were used for an efficient 3D acquisition.

Animal experiments were performed on normal mice and the transgenic adenocarcinoma of the mouse prostate (TRAMP) model with a dual-tuned mouse coil in a GE 3T scanner. In order to characterize the contrast, 3D MRSI with and without STE encoding were acquired in two separate experiments. Imaging was acquired 35 sec following the start of the 80 mM hyperpolarized [1-^{13}C]-pyruvate injection with 5x5x5.4mm resolution, 8x8x16 matrix size, TE = 20 - 140ms, TR = 75-215ms, progressive flip angles, concentric encoding, and a mixing time of 1-3 sec.

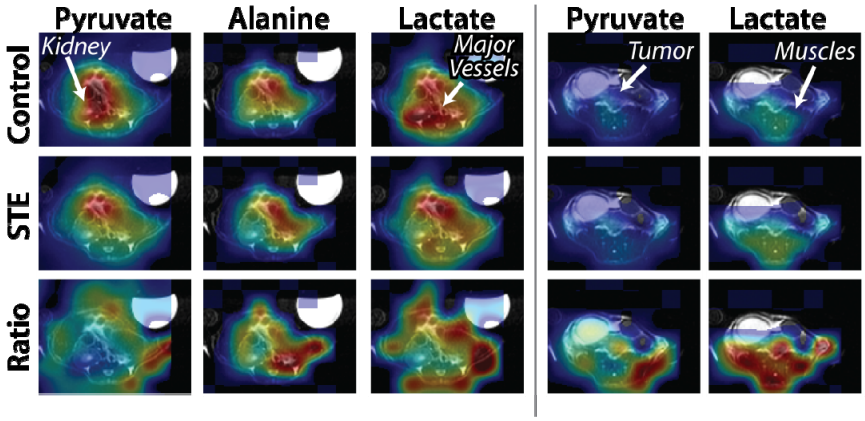

Figure 2: STE vs control maps in a TRAMP mouse, showing lac and pyr are highlighted in the tumor and muscle relative to the kidneys and vessels.

Results: Only a small fraction of the metabolite signal was retained in the kidneys, indicating most of the metabolites are flowing through the organ, and the STE showed no signal in the heart and chest. The liver metabolites demonstrated less mobility (especially ^{13}C-alanine with STE:control = 0.375 signal retained), and the prostate and prostate tumors were particularly highlighted, with average STE:control = 0.289 (pyruvate) and 0.399 (lactate). Metabolites in muscle voxels were also relatively well highlighted with the STE encoding. Overall, pyruvate was observed to have more mobility than lactate and alanine likely because it has a larger concentration in the blood.

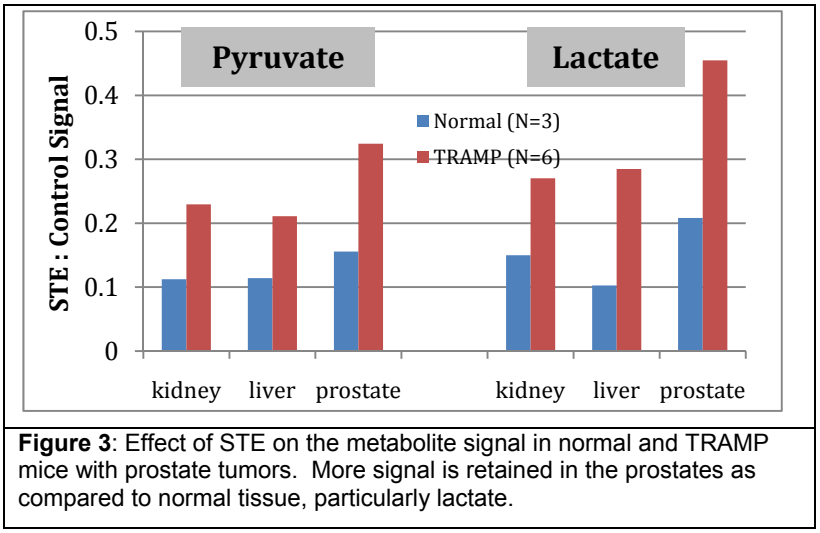

Figure 3: Effect of STE on the metabolite signal in normal and TRAMP mice with prostate tumors. More signal is retained in the prostates as compared to normal tissue, particularly lactate.

Discussion: The STE pulse sequence provided higher contrast-to-noise (CNR) for prostate cancers, while suppressing flowing metabolites, particularly in the heart and kidneys. This new approach demonstrates the ability to provide novel information about the local environment and metabolic state.

References: [1] Golman K, et al. PNAS 103(30): 11270-5 (2006). [2] Frahm J, et al. JMR 1985; 64: 81-93. [3] Larson PEZ, et al. ISMRM 2009, p. 2410. [4] Cunningham CH, et al. ISMRM 2009, p. 2422. [5] Chen AP, et al. JMR 2009; 200(2): 344-348. [6] Hennig J, Il'yasov KA, ISMRM 1998; 658. [7] Hennig J, et al, MRM 51:68-80 (2004).

Acknowledgments: Funding from NIH R01 EB007588 and American Cancer Society PF-09-036-01-CCE.